Proof of Concept Design for a Ultraviolet Spectropolarimeter CubeSat Platform: Low Cost Means of Studying the Magnetic Fields of the Solar Atmosphere

Ian Geraghty, Dawson Stokley, Zach Allen, Andrew Arnold, Caleb Beavers,
Joshua Bruski-Hyland, Darin Brock, Matthew Funk, Ryan Lynch, Mattew Normile, Andrew Lux
University of Colorado at Boulder, Aerospace Engineering Sciences, AIAA Student Members

Solar storms present a global threat to modern society because of their ability to disrupt power grids and satellite communications. As society becomes more technologically dependent, there is a growing need to understand and monitor solar activity. Polarimetry is a novel method for studying the Sun's magnetic field, which governs the explosive events that cause space weather on Earth. This technique relies on measuring light intensity as a function of polarization angle to deduce information regarding magnetic field structure. Polarimetric observations of the Sun have been made by several instruments, but little work has been done in the field of ultraviolet polarimetry. Ultraviolet radiation is emitted from the solar atmosphere, which is also the region where solar wind is driven and space weather is generated. Observations of the Sun in this spectral range could be of significant importance for identifying precursors of large scale solar events, as well as monitoring space weather. STOUT, the Spectropolarimeter Telescope Observatory for Ultraviolet Transmissions, is a 6U high-altitude balloon payload designed by University of Colorado Boulder aerospace engineering undergraduate students, as a proof of concept for a CubeSat spectropolarimeter platform. The instrument measures light intensity as a function of linear polarization over the 270 to 400 nm range and utilizes a field of view of 55.0" $\pm$ 0.1" so that small regions of the Sun can be observed independently. The instrument includes an internal pointing system, which allows measurements to be taken in two spatial dimensions. Based on modeling, the system provides a pointing accuracy of $\pm$ 2.75' in azimuth and $\pm$ 1.75' in elevation with 3 sigma confidence. The payload is planned to be flown by the University Corporation for Atmospheric Research High Altitude Observatory in Summer 2018.

Nomenclature

CME	=	Coronal Mass Ejection
d_{ap}	=	distance from cage gimbal to pointing apex
DOF	=	Degree of Freedom
FOV	=	Field of View
L_h	=	horizontal actuation distance
L_v	=	vertical actuation distance
NASA	=	National Aeronautics and Space Administration
ϕ	=	elevation angle
r_{apex}	=	position of apex
$r_{apex,hb}$	=	position vector, apex to horizontal ball joint
$r_{apex,vb}$	=	osition vector, apex to vertical ball joint
$r_{apex,hb,zero}$	=	zero angle position vector, apex to horizontal ball joint
$r_{apex,vb,zero}$	=	zero angle position vector, apex to vertical ball joint
$r_{apex,zero}$	=	zero angle apex position
r_{cg}	=	cage gimbal position
$r_{cg,hb}$	=	position vector, cage gimbal to horizontal ball joint
$r_{cg,vb}$	=	position vector, cage gimbal to vertical ball joint
r_{hg}	=	horizontal gimbal position
r_{vg}	=	vertical gimbal position
r_{hb}	=	horizontal ball joint position
r_{vb}	=	vertical ball joint position
RotMat	=	transformation matrix
SNR	=	Signal to Noise Ratio
STOUT	=	Spectropolarimeter Telescope Observatory for Ultraviolet Transmissions
θ	=	azimuth angle
UV	=	Ultraviolet

I. Introduction

The threat to modern infrastructure posed by extreme solar activity is unprecedented in our current age of technological reliance. Solar storms such as flares and coronal mass ejections (CMEs) cause charged particles to be projected from the Sun with increased energy such that they trigger geomagnetic storms on Earth. The influx of high energy particles associated with severe space weather events is capable of disrupting satellite telecommunications and power grids to the point of producing large-scale communication and power blackouts. These events also create high radiation environments that are dangerous to humans, aircraft, and spacecraft. For example, the effects of a solar event in 2003 caused the failure of power systems in Northern Europe, International Space Station astronauts to take shelter, flight paths to be rerouted, and possibly caused the loss of the ADEOS-2 satellite[3]. Solar storms of greater magnitude than the 2003 event have been recorded, the largest being the 1859 Carrington Event where the geomagnetic storm caused by a CME produced worldwide auroras and caused telegraphs to catch fire[5]. The impacts of such an event in the modern age could prove to be disastrous. Increasing awareness of the susceptibility of modern technology to space weather has spurred greater dedication to solar observations and space weather services, but the understanding of what causes solar activity is far from complete.

The common understanding is that eruptive solar events are caused by the release of stresses in the Sun's magnetic field[1]. Polarimetry has proved to be a novel technique for studying magnetic field structure. Light becomes polarized by the presence of a magnetic field due to the Zeeman and Hanle effects[4]. The polarization of light can be described by the Stokes parameters I, Q, U, and V which represent total intensity, vertical polarization, horizontal polarization, and circular polarization respectively[2]. Solar polarimetric observations rely on measurements of the Stokes parameters and the principles of the Zeeman and Hanle effects to infer knowledge of the structure and evolution of the Sunmagnetic field[4].

Polarimetric observations of the Sun by instruments such as the Advanced Stokes Polarimeter/ Diffraction Limited Spectropolarimeter, Spectropolarimeter for Infrared and Optical Regions, SOLIS VSM and the Hinode Solar Optical Telescope have contributed to many recent advancements in heliophysics[1]. Very little has been done in the area of ultraviolet (UV) polarimetry, primarily because of the need to use spaceborne instruments to avoid atmospheric scattering. UV light is primarily generated in the solar corona and transition region. Since this is the region where space weather is generated, this spectral range provides an ideal platform for studying extreme solar activity[4].

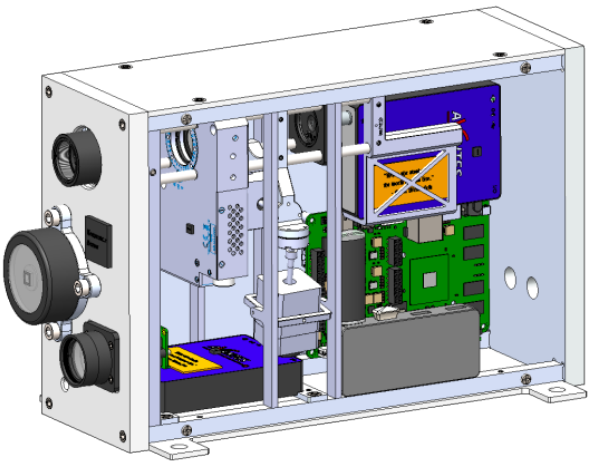

Figure 1. Fully assembled STOUT module

The Spectropolarimeter Telescope Observatory for Ultraviolet Transmissions (STOUT) instrument (Figure 1) is a high-altitude balloon payload designed as a proof of concept for a low-cost and reproducible CubeSat platform for studying and monitoring the solar atmosphere through polarimetric observations in the UV spectrum. This technology aims to advance the understanding of the physics of the solar atmosphere and possibly identify precursors of dangerous solar events. The optical system of the instrument is compromised of a small field of view (FOV) imager, a rotatable wire grid polarizer, and a spectrometer, which together are capable of measuring the Stokes parameters I, Q, and V. A pointing system was designed to actuate the optical system in order to make measurements at variable points on and around the Sun during a balloon flight. This paper will focus on the design of the optical and pointing systems.

II. Mission

The STOUT module is designed for flight on a National Aeronautics and Space Administration (NASA) high altitude balloon gondola with a cruise altitude of 40 km. The instrument will be mounted to the gondola by the four tabs seen in Figure 1 and will receive continuous power from on board batteries. While the gondola that will be used for STOUT's flight is undecided, for this project it is assumed that the gondola will have a attitude control system and point the module to within $\pm 5^{\circ}$ of the center of the Sun.

The flight is characterized by three distinct phases of ascent, cruise, and descent. The ascent phases lasts for approximately two hours during which the STOUT module begins monitoring pressure, humidity, and temperature.

During this phase the module also begins controlling internal temperature through the use of various pad heaters.

Solar UV spectra at variable polarization angles is collected once the gondola reaches 40 km and begins the two week cruise phase. The data collection procedure begins by determining the position of the Sun's center relative to the gondola's attitude. The azimuth and elevation angle of the Sun's center relative to the gondola is recorded by a quadrant photodector sensor mounted on the front face of the module. Once the linear actuators point the optical system at the Sun's center, the spectrometer takes a spectrum reading. This measurement is repeated as the rotating polarizer mount rotates the wire grid polarizer to eight different positions between 0° and 180° in 22.5° increments. Note that due to physical symmetries in polarization only measurements over 0° to 180° are needed for polarimetric studies. At this point the linear actuators point the optical system at a different point on the Sun and spectrum measurements are taken at the eight different polarization angles. The entire procedure is repeated until UV spectra of the whole Sun is collected at eight different polarization angles and the procedure restarts.

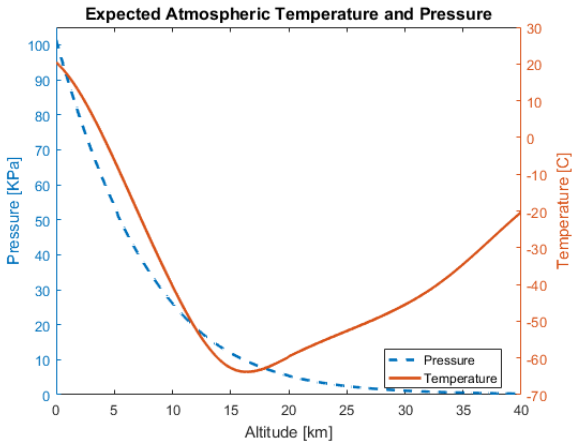

Figure 2. Standard Atmospheric Model Conditions of Launch Location Fort Sumner, NM

The descent phase lasts for only one hour. During this phase, the gondola detaches from the balloon and descends through the atmosphere under parachute. Once the gondola has impacted with the ground the collected data can be retrieved from the on board USB drives. For this project, only the exterior structure and USB's are designed to withstand the 5g impact with the ground.

The environmental conditions of a high altitude flight had to be considered in order to develop an instrument capable of operating in the extreme conditions. STOUT is designed to survive external temperatures of -70°C, as well as operate in an external temperature of -20° and a pressure of 10 Pa (Figure 2).

III. Optical System

The purpose of the optical system is to take spectrum measurements over the 270 nm to 400 nm spectral range at variable polarization angles. The development of this design was driven by the size constraints of the 6U CubeSat structure and the desire to have a linear optical path. An optical system with minimal dimensions is favorable because it provides more room for the system to move inside the module, thus increasing its possible pointing range. A linear optical path is ideal because it eliminates the need for mirrors or optical fibers, both of which could cause instrumental polarization of incoming light. Instrumental polarization is hard to characterize and could render the measurements collected by STOUT invalid.

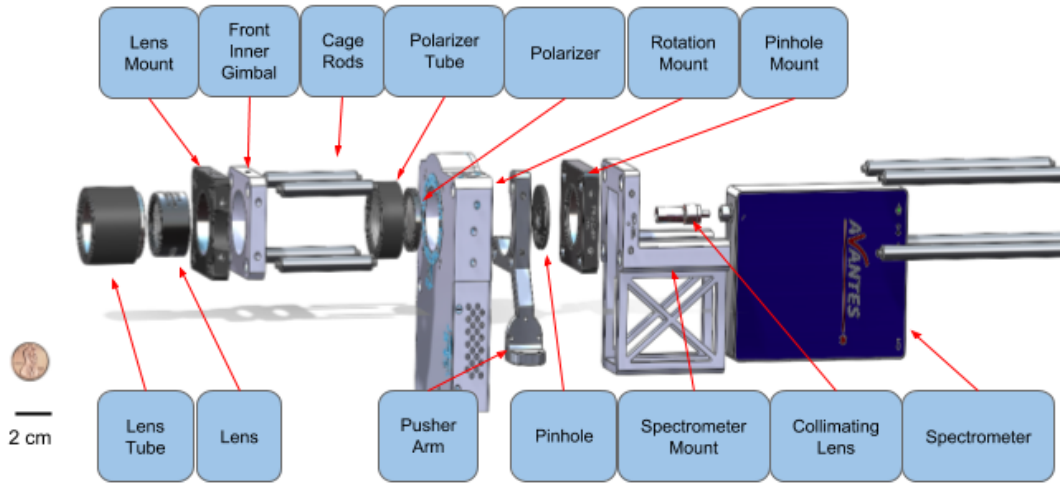

Figure 3. Exploded view of the STOUT optical system

Table 1 outlines the specific requirements that the optical system need to meet in order to maximize the scientific usefulness of the collected data.

Requirements	Criteria Met
Isolate a <= 60" spot in the system FOV	55.0"±0.1" FOV
Take spectrum measurements over the 270 - 400 nm range	270 - 426 nm spectral range
Rotate polarizer with <= 0.5° accuracy	± 0.14° rotational accuracy

Table 1. STOUT optical system design requirements

A. Lens

Light enters the optical system through a 25mm diameter Thorlabs Air-Spaced Achromatic Doublet lens with a focal length of 150 ± 1.5 mm. This lens is responsible for focusing incoming UV light into a coherent image. Since STOUT aims to observe a broad spectral range, an achromatic lens was chosen to minimize chromatic aberrations. Chromatic aberrations arise because different wavelengths have different indexes of refraction. This causes different wavelengths of light to come into focus at slightly different positions and results in an overall degradation of focusing quality. High focusing quality is necessary in order to effectively observe different portions of the Sun. Sampling from a blurry image would allow light from the Sun originating at different regions than the desired observation region to degrade spatial isolation.

B. Polarizer and Rotation Mount

Located between the lens and its focal plane is a Thorlabs Stepper Motor Rotation Mount equipped with a 25 mm diameter Thorlabs Ultra Broadband Wire Grid Polarizer. The diameter of the polarizer is the same as that of the focusing lens to ensure that all of the incoming light is polarized. The rotation mount has internal threading so that the polarizer can be secured inside the mount from each side via two retaining rings. The stepper motor rotation mount changes the orientation of the polarizer and effectively controls the polarization angle of the input light with an accuracy of ±0.14°. Since the optical system doesn't include components besides the polarizer that induce any sort of polarization, the total polarization angle accuracy of the system is defined by the accuracy of the rotation mount.

C. Pinhole

A 40 ± 3 μm diameter Thorlabs Precision Pinhole is located in the focal plane of the lens. The pinhole drastically reduces the FOV of the optics system so that small regions of the Sun can be observed independently. The system's FOV is dependent on the focal length of the focusing lens and the diameter of the pinhole. With the chosen lens and pinhole size the optical system's FOV is found to be 55.0 ± 0.1".

$$\theta = 2 * arctan(\frac{d}{2 * f}) = 0.0153^\circ = 55.0"$$

$$\delta\theta = \sqrt{(\frac{\partial\theta}{\partial f} * \delta f)^2 + (\frac{\partial\theta}{\partial d} * \delta d)^2} = (2 * 10^{-5})^\circ = 0.1"$$

Once the system's FOV was characterized the optical design software, Zemax, was used to model the focusing quality of the lens. In the model 270, 335, and 400 nm light rays enter the system at angles of ± 27.5" in azimuth and elevation and 0°. These rays represent light entering the system from the outer perimeter of the FOV. Figure 4 below shows the focused rays at the lens's focal length.

Diffraction effects cause the focused rays to broaden but the centers of the rays correspond to positions on the circumference of the pinhole, which validates the FOV calculations. The total energy of the centered ray falls within the pinhole area indicating that the achieved focusing quality is sufficient for STOUT's purposes.

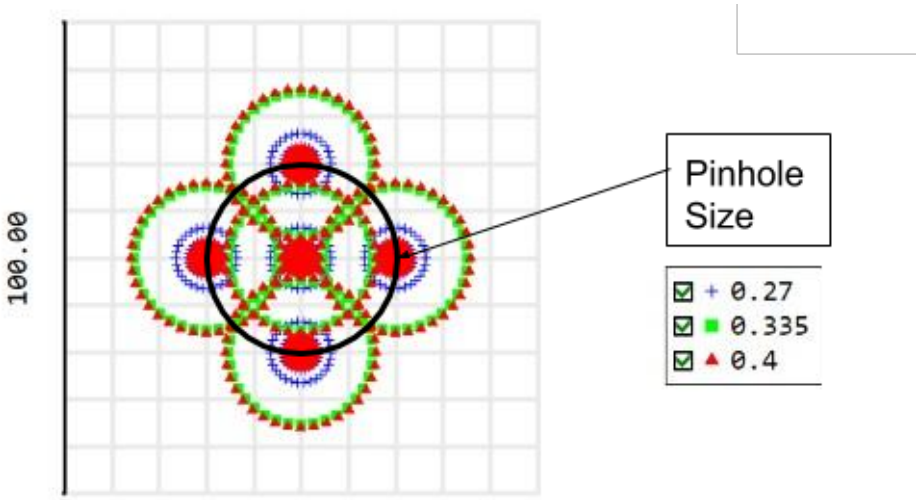

Figure 4. Spot diagram of focused light rays from the optical system FOV. All units are in μm and the legend refers to the wavelengths of light modeled.

D. Spectrometer

Located directly behind the pinhole is an Avantes AvaSpec-Mini spectrometer affixed with a 6 mm diameter collimating lens. Once the incoming light is focused, polarized, and spatially filtered it passes through the spectrometer's collimating lens and into the spectrometer which records the light's spectra. The collimating lens acts to bend the light that passes through the pinhole such that the rays are travelling parallel to one another. This increases the amount of light able to pass through the spectrometer aperture. Avantes software provides an option to autoset the exposure time to maximize the data signal to noise ratio (SNR) and will be used during STOUT's flight. Intensity measurements are normalized by the spectrometer's CCD maximum photon count so variable exposure times will not effect the collected data.

E. Mounting Hardware

The components of the optical system are mounted using a Thorlabs Optics Cage System, which allows for easy integration of the various optical components. This mounting system is compromised of square cage plates with internal threading mounted to four perpendicular stainless steel rods via set screws.

The focusing lens is secured in a threaded lens tube with retaining rings and screwed into a cage plate. The tube containing the lens also acts as a baffling system to minimize the amount of stray light entering the system. The pinhole is secured directly inside of a cage plate from both sides by two retaining rings. The rotating polarizer mount also has four threaded holes that allow cage rods to be secured to the rotating mount. The mount that integrates the spectrometer with the optics cage is the only piece of the optics system that is not commercially available. This mount is attached to the optics system via the four cage rods and was 3D printed out of Formlabs Engineering Tough material. The mount was baked in a vacuum chamber to minimize outgassing that would otherwise happen during the flight.

Additional lens tubes were included that extend from the back of the focusing lens to the rotating mount, from the back of the rotating mount to the pinhole, and from the pinhole to the body of the spectrometer. These lens tubes act as a light seal and ensure that the light entering the spectrometer is originating from the optical system FOV. These components minimize stray light from cracks in the STOUT structure or the LED's on the various electronic components inside STOUT.

IV. Pointing System

The pointing system is responsible for pointing the optical system at various different positions on the Sun. The pointing system needs to have pointing capabilities in azimuth and elevation to perform the desired scan of the entire Sun. The system must also be able to point over a considerable range so that measurements can be taken when the balloon gondola is not pointing the instrument directly at the Sun. The design requirements for the STOUT pointing system include an azimuth pointing range of $\pm 5^\circ$ and an elevation pointing range of $\pm 1^\circ$. Commercial platforms that provide such pointing capabilities are available but the costs significantly exceed the STOUT project budget; therefore, a custom solution was developed. The pointing system design was influenced by the need for arcminute accuracy and the size constraints of the CubeSat structure.

The preliminary design involved a static optics cage to mount the lens, polarizer, rotating mount, and spectrometer. The pinhole itself would then be actuated vertically and horizontally throughout the focal plane by two linear actuators. However, Zemax modeling showed that the degradation of focusing quality in the extremes of the lens' FOV would be enough to make the effective isolation of a particular region of the Sun impossible. This is caused by spherical abberations that arise from the lens geometry. The solution was to develop a design that allowed for a non-static optical system with two rotational degrees of freedom (DOF).

The design is based upon a gimbal-like mount for the front of the optics cage that allows for azimuth and elevation rotation. The use of such a mount allows for the module's structure to remain closed in order to ease thermal management of the various electronic components. However, in such a mount the optics cage moves along an arc, which makes using linear actuators troublesome. To address this problem, motor casings were designed to hold two linear actuators which are mounted vertically and horizontally inside the STOUT module. The motors and motor casings are also mounted in two gimbal-like mounts that allow for azimuth and elevation rotation. A pusher arm was designed to be secured to the optics cage system via set screws, similar to the Thorlabs cage plates. The pusher arm has an appendage protruding diagonally from the corner of the optics cage to which two precision ball joints mounted vertically and horizontally on the pusher arm appendage are mounted. These ball joints act as contact points for the leads of the linear actuators. The rotation of the two motor gimbals and the pusher arm ball joints provide the freedom needed to move the optics cage along an arc using linear actuators. Excluding the linear actuators and ball joints, all of the components of the pointing system were manufactured out of aluminum 6061 by the STOUT team.

The STOUT pointing system needs to have an accuracy on the order of arcminutes in order to point from one location on the Sun to the other. To address this requirement multiple precautions were taken to minimize slack in the custom-made components that could result in errors in the desired pointing angle.

A. Pusher Arm and Ball Joints

The pusher arm is mounted to the optical cage system via set screws between the rotating polarizer mount and the pinhole. The appendage extending diagonally from the pusher arm has two surfaces to which two Myostat spherical rolling joints are mounted. These ball joints are connected to the linear actuator heads via female to female joints. The ball joints were selected because they are manufactured with high precision and are designed to have only 2.5 μm of slack in the joint.

B. Linear Actuators

Two Haydon Kerk Pittman Hybrid Stepper Motors are used to actuate the optical system. These motors were chosen because of their small dimensions and step size. The motors have encoders and a step size of 1.5 μm which allows the STOUT pointing system to accurately change its angular position by arcminutes at a time.

C. Motor Casings

Custom motor casings were designed to hold the linear actuators and integrate them with the gimbal-like mounts. The motors slide into the motor casings and are secured using four screws that thread through the back of the motor casing into screw holes in the motors themselves. There are holes on the top and bottom surfaces of the casings for pins that are used to integrate the casings and the gimbal mounts.

D. Optics Train Gimbal Mount

This mount sits directly behind the focusing lens cage plate and secures the optics train in place while providing two rotational DOFs. This mount consists of two hollow, concentric square plates. The outer plate has needle roller bearings press fit into the vertical sides that accept stationary pins which protrude horizontally from two vertical struts in the STOUT structure. These needle roller bearings provide elevation rotational freedom. This plate also has stationary pins protruding vertically from the top and bottom of surfaces. These pins fit into needle roller bearings that are press fit into the vertical faces of the inner plate, which provide the azimuth rotational freedom. The inner plate of the mount is secured onto the rods of the optics cage using set screws. Teflon washers are placed between the pins that connect the inner and outer plates and the pins that connect the outer plate to the vertical struts. The washers act to minimize slack in the bearings of each component while allowing the mounts to rotate freely because of teflon's low frictional properties.

E. Motor Gimbal Mounts

The gimbal mounts for the horizontal and vertical motors are very similar to that of the optics train gimbal mount. They consist of a single hollow plate with needle roller bearings press fit into the vertical faces. These bearings accept stationary pins that protrude from the motor casings and provide azimuth rotational freedom. The plate also has needle roller bearings press fit into the horizontal faces which accept stationary pins from vertical struts in the STOUT structure to provide elevation rotational freedom. Teflon washers were placed between the motor casings and the plate, as well as the plate and the vertical struts to minimize slack in the bearings.

F. Pointing Equation Derivation

This section defines the equations used to relate the desired pointing angle to the actuation required from the vertical and horizontal actuators. This is the algorithm that STOUT's flight computer will use to control the pointing system.Visual representations of the various parameters in the pointing angle derivation are shown in Figure 5.

Input values are the desired azimuth and elevation pointing angles of the optical system. Known values include the positions of the center of the optics cage gimbal mount, the two motor gimbal mounts, and the pusher arm. Also known are the locations of the center of the ball joints mounted to the pusher arm. These values were determined from the STOUT CAD model from which the complete instrument will be assembled. The center of the optics cage gimbal mount is taken to be the origin and then center of the pusher arm relative to the optics cage is referred to as the apex.

1. Values to Calculate

L_v and L_h

2. Known Values

θ, ϕ, r_{cg}, r_{vg}, r_{hg}, r_{vb}, r_{hb}, d_{ap}

3. Solution

First the vectors from the apex to the ball joint centers at 0^o azimuth and elevation angle are calculated. Note that the following vectors are in spherical coordinates.

$$\begin{aligned} r_{apex,zero} &= r_{cg} - (0, 0, d_{ap}) \\ r_{apex,vb,zero} &= r_{vb} - r_{apex,zero} \\ r_{apex,hb,zero} &= h_{hb} - r_{apex,zero} \end{aligned}$$

Then a coordinate transformation is required in order to convert the inputted spherical coordinates into cartesian coordinates. In Equation (1), the transformation matrix is multiplied by d_{ap} in order to find the location of the apex in its actual position (r_{apex}).

$$r_{apex} = \begin{pmatrix} -\sin(\theta) * \cos(\phi) \\ \sin(\phi) \\ -\cos(\theta) * \cos(\phi) \end{pmatrix} * d_{ap} \tag{1}$$

Another coordinate transformation is required to move into the optical cage gimbal mount frame. This is accomplished by creating a rotation matrix seen in Equation (2), and then performing a coordinate transform seen in Equation (3).

$$RotMat = \begin{pmatrix} \cos(\theta) & \sin(\theta) * \sin(phi) & \sin(\theta)\cos(\phi) \\ 0 & \cos(\phi) & -\sin(\phi) \\ -\sin(\theta) & \cos(\theta) * \sin(\phi) & \cos(\phi) * \cos(\theta) \end{pmatrix} \tag{2}$$

$$\begin{aligned} r_{apex,vb} &= RotMat * r_{apex,vb,zero} \\ r_{apex,bh} &= RotMat * r_{apex,hb,zero} \end{aligned} \tag{3}$$

At this point the positions of the actuated position of the ball joints can be calculated.

$$r_{cg,vb} = r_{apex,vb} + r_{apex}$$
$$r_{cg,hb} = r_{apex,hb} + r_{apex}$$

The actuation lengths of the vertical and horizontal stepper motors are calculated by taking the magnitude of the distance between the ball joints and the motor gimbal mounts. Half of the length of the motor is subtracted from these values due to the fact that the motor head does not sit in the center of the motor mount when completely retracted.

$$L_v = Norm[r_{cg,vb} - r_{vg}] - \frac{L_{motor}}{2}$$
$$L_h = Norm[r_{cg,hb} - r_{hg}] - \frac{L_{motor}}{2}$$

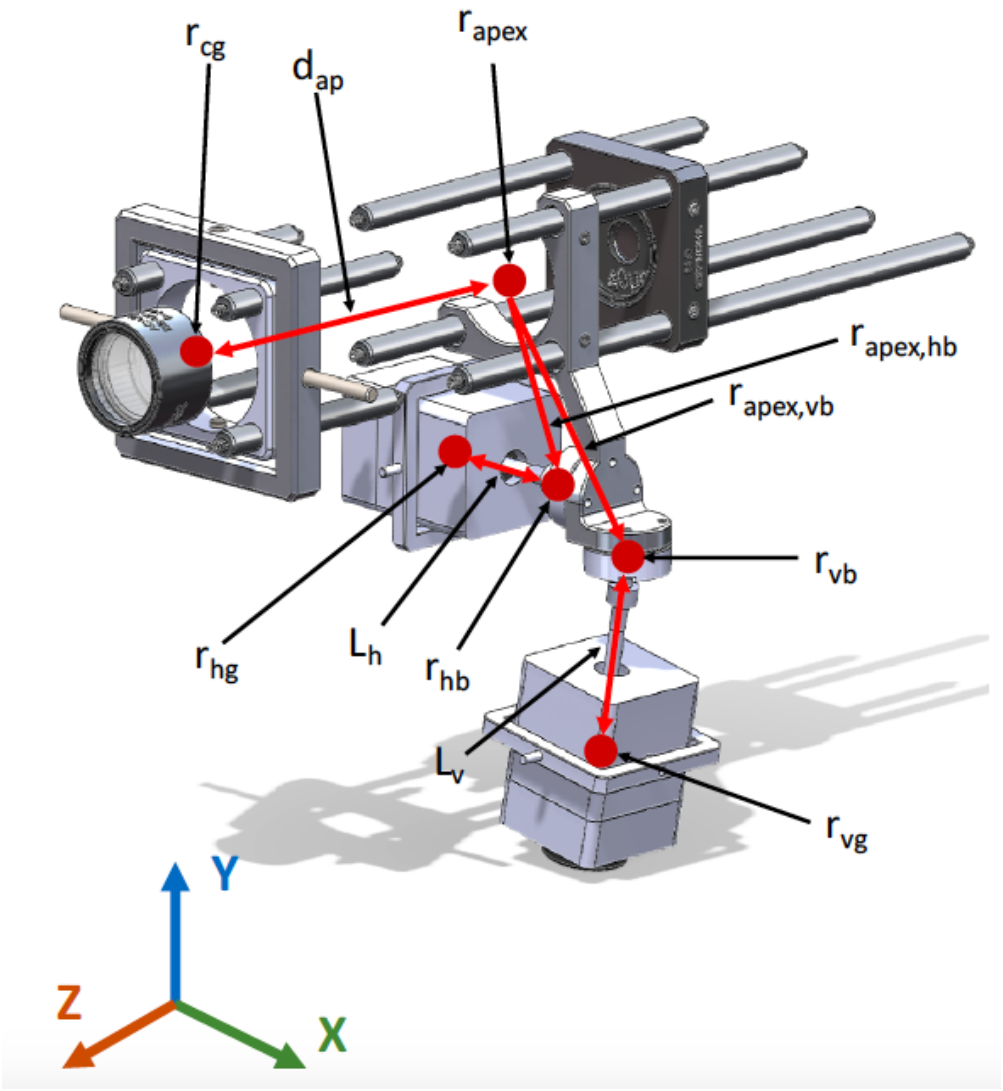

Figure 5. Visual representation of parameters in the pointing algorithm

G. Pointing Error Monte Carlo Model

The accuracy of the pointing system is dependent on the slack in the three gimbal mounts and the the ball joints. Table 2 shows the estimations of these values. Note that the slack values for the ball joints are certified by their manufacturer, and perform better than the design values.

Component	X-slack (μm)	Y-slack (μm)	Z-slack (μm)
Cage Gimbal	$\pm$5	$\pm$10	$\pm$5
Motor Gimbals	$\pm$5	$\pm$10	$\pm$5
Ball Joints	$\pm$1	$\pm$1	$\pm$1

Table 2. Cartesian coordinate estimates of slack in pointing system hardware

Straight forward error analysis of this pointing system cannot be performed because of the multiple rotational degrees of freedom of the gimbal mounts. Incorporating the slack into the pointing equations makes the system unconstrained and therefore unsolvable. In order to roughly characterize the error of the pointing system a Monte Carlo simulation was performed. In this simulation the total amount of slack in the system from the ball joints and gimbal points is applied as purely vertical and horizontal perturbations of the apex position. This represents a worst case scenario because in actuality the slack of each component will effect the apex position as a function of the sine of the angle of the motors. The simulation involves drawing random values from a normal distribution with a one σ value equivalent to the slack of the respective component, and a mean value of zero. This is done for each component and compounded into a total error in the position of the apex position. Additional constraints were put on the simulated slack values to account for the effects of gravity. In order to further overestimate the total pointing error of the system we take the 3σ simulation values as the azimuth and elevation pointing angles. This results in an azimuth pointing angle error of $\pm$ 2.75' and an elevation pointing angle error of $\pm$ 1.75'.

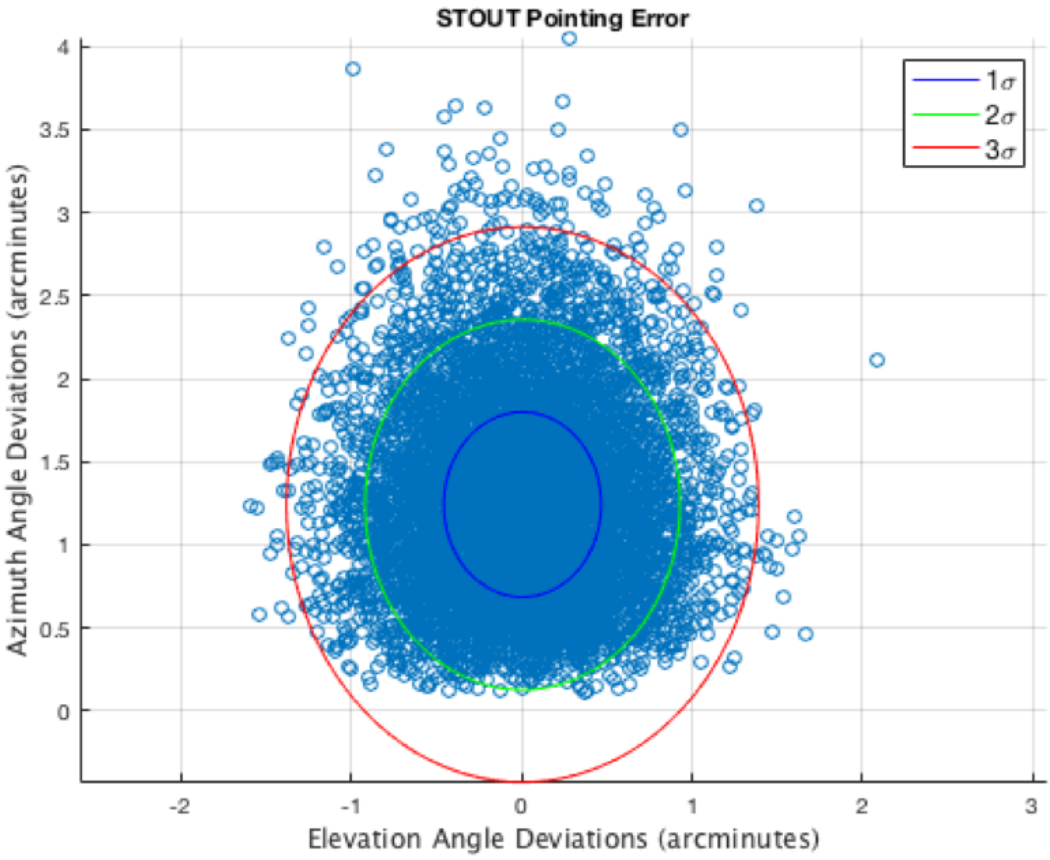

Figure 6. Results of monte carlo simulation of pointing error

V. Conclusion

Through the use of a simple optical system and a high accuracy pointing system the STOUT instrument demonstrates the technology needed to fill the data gap that exists in the field of UV polarimetry for less than $8000. The optical system has the ability to take high SNR UV spectrum measurements at variable polarization angles with a

polarization angle accuracy of $\pm$ 0.14°. With a FOV of 55.0" $\pm$ 0.1", the system is capable of observing small regions of the Sun at a time. The pointing system has the ability to point the optical system over an azimuth range of $\pm$5° and an elevation range of $\pm$1° with an accuracy of $\pm$ 2.75' and $\pm$ 1.75', respectively. The integration of these two systems results in an instrument capable of scanning the Sun while recording high temporal resolution measurements of variable polarization angle UV spectra. This data can be used to study the evolution of the Sun's magnetic field structure and provide a useful tool for studying the precursors of extreme solar activity that results in geomagnetic storms on Earth.

Other subsystems of the STOUT instrument not discussed in this paper include an attitude determination system, an environmental control system, a power distribution system, as well as a control and data acquisition system. These systems are critical for making the STOUT instrument flight ready. The attitude determination system detects where the Sun is relative to STOUT and provides feedback for the pointing system so that it can accurately perform a scan of the Sun. The environmental control system keeps all of the electronic components at operable temperatures in the extremely cold temperatures of the middle atmosphere. The power distribution system is designed to allocate power from balloon gondola battery packs to the various electronic components onboard STOUT. The control and data acquisition system manages the feedback control of the pointing system and environmental control system. This system is also responsible for saving data from all of the subsystems to the USB drives onboard STOUT.

The combination of these subsystems is an autonomous 6U high altitude balloon payload. The fully assembled instrument has a total mass of 4.4 kg and draws a maximum power of 74.5 W. This technology will be used as proof of concept design for what could ultimately be a CubeSat constellation with the purpose of studying the magnetic fields of the Sun's corona and transition region. As of this writing, the STOUT instrument is in the final stages of assembly and the STOUT team is preparing for a rigorous testing schedule. The planned tests include thermal vaccum chamber testing to validate the performance of the instrument's environmental control system and a calibration campaign. For the calibration campaign, the instrument will be mounted onto the University of Colorado's Sommers-Bausch Telescope. This telescope has a pointing accuracy of 20" and will be used to calibrate STOUT's attitude determination and pointing systems. This campaign will also be used to verify the accuracy of the pointing system and to evaluate the response time of the pointing system to an external perturbation in attitude.

Acknowledgements

The STOUT team would like to thank everybody that contributed to the success of the STOUT project. We sincerely appreciate the assistance and guidance from our faculty advisor Dr. Fransisco Lopez-Jiminez. We'd like to thank our customers Phil Oakley and Scott Sewell from the UCAR High Altitude Observatory for all their guidance and support, as well as letting us use their thermal vaccum chamber for testing. We'd like to thank Matt Rhode and Adrian Stang for his invaluable technical assistance during the design and manufacturing process. We'd like to thank Trudy Schwartz and Bobby Hodgkinson, for their great technical assistance and the use of their lab spaces. We'd like to thank the Sommers-Bausch Observatory Operations Manager, Fabio Mezzalira, for letting us use the Sommers-Bausch Telescope for testing and training us on its operation. We'd also like to thank the other faculty on the Project Advisory Board and our course assistants for their reviews and input on our project: Dr. Dale Lawrence, Dr. Jelliffe Jackson, Dr. Torin Clark, Dr. Donna Gerren, Dr. Zoltan Sternovsky, Dr. Jade Morton, Lee Huynh, and Timothy Kiley. Finally, we'd like to thank the Engineering Excellence Fund for expanding our project budget by $2377. Without these extra funds, descoping our project was inevitable. We are extremely happy with the results of our project and none of it would have been possible without the support of all those who were mentioned.

References

[1] *Causes of Solar Activity: A Science White Paper for the Heliophysics 2010 Decadal Survey*. PDF. National Solar Observatory. (Visited on 02/13/2018).

[2] *Imaging Spectropolarimeter for Multi-application Solar Telescope at Udaipur Solar Observatory: Characterization of polarimeter and preliminary observations*. PDF. National Solar Observatory. (Visited on 02/18/2018).

[3] Division on Engineering Space Studies Board and National Research Council Physical Sciences. *Severe Space Weather Events: Understanding societal and economic impacts*. PDF. Committee of the Societal and Economic Impacts of Severe Space Weather Events. (Visited on 02/15/2018).

[4] Jan O. Stenflo. *Stokes Polarimetry of the Zeeman and Hanle Effects*. PDF. (Visited on 02/13/2018).

[5] Joseph Stromberg. *What Damage Could be Caused by a Massive Solar Storm*. Web Article. Smithsonian.com. (Visited on 02/15/2018).